

Generation and Characterization of ALX-0171, a Potent Novel Therapeutic Nanobody for the Treatment of Respiratory Syncytial Virus Infection

Laurent Detalle,^a Thomas Stohr,^{a*} Concepción Palomo,^e Pedro A. Piedra,^{b,c} Brian E. Gilbert,^b Vicente Mas,^e Andrena Millar,^d Ultan F. Power,^d Cateljine Stortelers,^a Koen Allosery,^a José A. Melero,^e Erik Depla^a

Ablynx nv, Zwijnaarde, Belgium^a; Department of Molecular Virology and Microbiology^b and Department of Pediatrics,^c Baylor College of Medicine, Houston, Texas, USA; Centre for Infection and Immunity, School of Medicine, Dentistry and Biomedical Sciences, Queen's University Belfast, Belfast, Northern Ireland, United Kingdom^d; Centro Nacional de Microbiología and CIBER de Enfermedades Respiratorias, Instituto de Salud Carlos III, Madrid, Spain^e

Respiratory syncytial virus (RSV) is an important causative agent of lower respiratory tract infections in infants and elderly individuals. Its fusion (F) protein is critical for virus infection. It is targeted by several investigational antivirals and by palivizumab, a humanized monoclonal antibody used prophylactically in infants considered at high risk of severe RSV disease. ALX-0171 is a trimeric Nanobody that binds the antigenic site II of RSV F protein with subnanomolar affinity. ALX-0171 demonstrated *in vitro* neutralization superior to that of palivizumab against prototypic RSV subtype A and B strains. Moreover, ALX-0171 completely blocked replication to below the limit of detection for 87% of the viruses tested, whereas palivizumab did so for 18% of the viruses tested at a fixed concentration. Importantly, ALX-0171 was highly effective in reducing both nasal and lung RSV titers when delivered prophylactically or therapeutically directly to the lungs of cotton rats. ALX-0171 represents a potent novel antiviral compound with significant potential to treat RSV-mediated disease.

Human respiratory syncytial virus (RSV) is the most important viral pathogen causing acute lower respiratory tract infections in infants worldwide and is estimated to result in ~3.4 million yearly hospitalizations and ~200,000 deaths globally (1). RSV typically causes its primary infection at the point of entry: apical ciliated epithelial cells that line the nasal cavity and airways (2, 3). Primary infections are usually symptomatic, with clinical signs ranging from mild upper respiratory tract illness to severe lower respiratory tract infections, including pneumonia and bronchiolitis (4). In addition to the acute consequences of infection, the development of long-term recurrent wheezing and asthma has been associated with severe RSV infections in infancy (5, 6). Despite the major clinical importance of RSV, no vaccines or widely accepted antiviral therapies are currently available. The only available drug specific for human RSV is palivizumab (Synagis), a marketed monoclonal antibody that is administered prophylactically before and during the RSV season to infants at high risk of having severe human RSV disease (7–9). Its use is restricted to premature infants (gestational age, <29 weeks), if they have no other underlying morbidities, and infants with chronic lung disease, congenital heart disease, or a compromised immune system during the first year of life (10).

RSV is a member of the *Pneumovirus* genus of the *Paramyxoviridae* family and has a linear single-stranded, nonsegmented RNA molecule of negative polarity as its genome. This genome contains 10 genes which encode 11 proteins. The transmembrane glycoproteins F and G are the primary surface antigens of RSV. The attachment (G) protein mediates binding to cell receptors, while the F protein promotes fusion of the viral and cell membranes, allowing virus entry into the host cell cytoplasm (11). The F protein also promotes the fusion of infected cells with adjacent uninfected cells, facilitating the formation of multinucleated cell formations (syncytia), which allow cell-to-cell transmission of the

replicated viral RNA and confer additional protection for the virus against host immune responses (12).

On the basis of the antigenic and genetic variability of the G protein, two subgroups of RSV (subgroups A [RSV-A] and B [RSV-B]) have been identified, and these are composed of evolving genotypes (13–17). In contrast to the G protein, the F protein is mostly conserved between RSV subgroups A and B (89% amino acid identity) and is therefore considered the most promising target for the development of viral entry inhibitors.

Nanobodies are therapeutic proteins derived from the heavy-chain variable domains (VHH) that occur naturally in heavy chain-only immunoglobulins of the *Camelidae* (18, 19). The formatting flexibility of Nanobodies into multivalent constructs, their small size, their stability (which allows delivery through nebulization), and their ease of production make their use against viral targets appealing (20–22).

Received 31 July 2015 Returned for modification 19 August 2015

Accepted 25 September 2015

Accepted manuscript posted online 5 October 2015

Citation Detalle L, Stohr T, Palomo C, Piedra PA, Gilbert BE, Mas V, Millar A, Power UF, Stortelers C, Allosery K, Melero JA, Depla E. 2016. Generation and characterization of ALX-0171, a potent novel therapeutic Nanobody for the treatment of respiratory syncytial virus infection. *Antimicrob Agents Chemother* 60:6–13. doi:10.1128/AAC.01802-15.

Address correspondence to Laurent Detalle, Laurent.detalles@ablynx.com.

* Present address: Thomas Stohr, A2M Pharma GmbH, Monheim, Germany.

Supplemental material for this article may be found at <http://dx.doi.org/10.1128/AAC.01802-15>.

Copyright © 2015 Detalle et al. This is an open-access article distributed under the terms of the [Creative Commons Attribution-Noncommercial-ShareAlike 3.0 Unported license](https://creativecommons.org/licenses/by-nc-sa/4.0/), which permits unrestricted noncommercial use, distribution, and reproduction in any medium, provided the original author and source are credited.

Here we describe the *in vitro* and *in vivo* characterization of ALX-0171, a trivalent Nanobody composed of three monovalent Nb017 moieties linked together with glycine-serine (GS) linkers which is designed to target the RSV F protein for delivery via inhalation. ALX-0171 is currently in clinical development for the treatment of RSV infections in infants (23).

MATERIALS AND METHODS

Generation of RSV-specific Nanobodies. Monovalent RSV F protein-specific Nanobodies were identified from immune libraries of llamas that received repetitive injections with soluble recombinant F protein (F_{TM} -NN protein), inactivated RSV-A (catalog number 8RSV79; HyTest), or a combination of both antigens. The soluble recombinant form of the F protein (derived from the Long strain) was produced with recombinant Sendai virus in embryonated eggs (24). RSV-neutralizing Nanobodies were identified by screening 162 distinct clones in an *in vitro* microneutralization assay with RSV subtype A Long on HEp-2 cells. RSV-neutralizing Nanobodies were formatted into multivalent constructs by genetic fusion with flexible Gly-Ser (GS) linkers of different lengths. Monovalent RSV Nanobody was routinely generated as C-terminal c-myc-His-tagged proteins in *Escherichia coli* (22). For the production of untagged monovalent and trivalent Nanobody constructs, a *Pichia pastoris* X-33 expression system was used (see Fig. S1 in the supplemental material). ALX-0171 is a trimeric Nanobody consisting of three RSV-targeting Nb017 subunits linked by two GS linkers.

Competition enzyme-linked immunosorbent assay (ELISA). Ninety-six-well microtiter plates (MaxiSorp immunoplates; Nunc) were coated overnight with inactivated RSV-A (HyTest) at 3.5 μ g/ml in bicarbonate buffer. The plates were blocked for 1 h with SuperBlock T20 (phosphate-buffered saline [PBS]) blocking buffer (Pierce) before being washed 3 times with PBS–0.05% Tween 20. Dilutions of ALX-0171 or palivizumab were mixed with 10 nM biotinylated ALX-0171 (1:1 ratio) and immediately transferred to the plates. After overnight incubation at room temperature (RT) and appropriate washing, a 1/3,000 dilution of peroxidase-labeled streptavidin (Thermo Scientific) was added to the plates for 1 h at RT. Bound streptavidin-horseradish peroxidase was revealed by adding 100 μ l/well of enhanced soluble tetramethylbenzidine (esTMB; SDT Reagents) for 10 min, followed by 1 N HCl. The absorbance was read at 450 nm, and the reference wavelength was 620 nm.

SPR. Affinity constants (the equilibrium dissociation constants [K_D]) of Nb017, ALX-0171, and palivizumab were determined by surface plasmon resonance (SPR) analysis on a Biacore X100 instrument (GE Healthcare). Fab fragments of antigenic site \emptyset -specific human monoclonal antibody (Mab) D25 (Fab D25) (25, 26) and antigenic site I-specific mouse Mab 2F (Fab 2F) (27) were used as controls. In brief, anti-His monoclonal antibody (GE Healthcare) was amine coupled to a CM5 sensor chip at a density of 12,000 to 13,000 resonance units (RU) in 10 mM acetate buffer, pH 4.5. Approximately 70 RU of His-tagged prefusion F protein was then bound to the anti-His monoclonal antibody. Compounds (ALX-0171, Nb017, Fab D25, Fab 2F, and palivizumab) were injected at 5 different concentrations (1 to 16 nM for ALX-0171, 8 to 128 nM for Nb017, 4 to 64 nM for palivizumab, 1.25 to 20 nM for Fab 2F and Fab D25) at a flow rate of 30 μ l/min. The association and dissociation phases were 2 and 13 min, respectively (for Fab D25, the dissociation time was increased to 30 min). The chip was regenerated using 10 mM glycine, pH 1.5. Different concentrations of the compounds were used to generate binding curves, which were fitted to a 1:1 Langmuir binding model for the calculation of the kinetic parameters association rate (k_{on}) and dissociation rate (k_{off}). The K_D was then calculated as the ratio of these two rate constants (k_{off}/k_{on}).

Binding of Nanobodies to RSV escape mutant F protein. HEp-2 cells grown in 100-mm-diameter plates were infected with either wild-type RSV (the RSV Long strain) or previously described mutant viruses resistant to neutralization by monoclonal antibodies (11, 28, 29) (multiplicity of infection, 1 to 3 PFU/cell). After 48 h, the cells were harvested and extracts were made in 500 μ l buffer/plate (the buffer was 10 mM Tris-HCl,

pH 7.5, 150 mM NaCl, 5 mM EDTA, and 1% octyl-glucoside). Equal amounts of each extract (50 μ l of a 1:500 dilution in PBS) were used to coat 96-well microtiter plates overnight at 4°C. The wells were saturated with 1% bovine serum albumin in PBS for 1 h, and after washing with PBS, Nanobodies were added to the wells and the plates were incubated for 1 h at RT. After washing, bound Nanobody was detected with a 1:1,000 dilution of rabbit anti-llama IgG antibody, followed by a 1:200 dilution of peroxidase-conjugated donkey anti-rabbit polyclonal antibody. *o*-Phenylenediamine dihydrochloride (OPD; Sigma) was used as the substrate, and reactions were stopped with 3 N H_2SO_4 , after which the absorbance at 490 nm was measured.

RSV clinical strains. Original clinical isolates of RSV-A and RSV-B strains were selected from the RSV bank at the Baylor College of Medicine (Houston, TX). Three additional RSV-A isolates (BT2a, BT3a, BT4a) were isolated from infants hospitalized with bronchiolitis in the Royal Belfast Hospital for Sick Children. This study was approved by The Office for Research Ethics Committees Northern Ireland (ORECNI). Written informed parental consent was obtained. They were all isolated and cultured in HEp-2 cells, as previously described (30, 31).

Antiviral assays. The neutralization activity of the selected Nanobodies and palivizumab was measured in a microneutralization assay, a neutralization assay, and a plaque reduction assay. They were performed using HEp-2 cell monolayers, as described in the supplemental material.

Cotton rat studies. Male and female cotton rats were bred and housed in the Baylor College of Medicine's vivarium in cages covered with barrier filters and given food and water *ad libitum*. Cotton rats weighing between 60 to 125 g were lightly anesthetized with isoflurane and intranasally challenged with 100 μ l of 1.41×10^5 to 3.5×10^5 PFU of RSV Tracy, depending on the experiment. RSV Tracy stocks were grown in HEp-2 cells. All the experimental protocols were approved by the Baylor College of Medicine Investigational Animal Care and Use Committee.

ALX-0171 was administered either intranasally or by nebulization. For intranasal administration, cotton rats were lightly anesthetized with isoflurane and inoculated intranasally with 100 μ l of ALX-0171.

For nebulization, an Akita² Apixneb nebulizer (Vectura GmbH, Germany) was used for whole-body exposure (see Fig. S2 in the supplemental material).

Cotton rats were euthanized with CO₂ at 4 days postinfection. The large left lobe and one of the large right lobes of the lungs were removed, rinsed in sterile water, and weighed. The left lobe was then transpleurally lavaged using 3 ml of Iscove's medium with 15% glycerol mixed with 2% fetal bovine serum (FBS)–minimal essential medium (MEM) (1:1, vol/vol) in a 3-ml syringe with a 26-gauge by 3/8-in. needle and injected at multiple sites to totally inflate the lobe. Subsequently, the lavage fluid was recovered by gently pressing the inflated lobe flat and further used to transpleurally lavage the right lobe following the same technique. The lavage fluid was collected and stored on ice until titrated. To obtain nasal washes, the jaws were disarticulated, the head was removed, and 1 ml of Iscove's medium with 15% glycerol mixed with 2% FBS–MEM (1:1, vol/vol) was pushed through each nare (total, 2 ml). The effluent was collected from the posterior opening of the pallet and stored on ice until titrated. RSV Tracy lung lavage titers and nasal wash titers were determined by plaque assay as described in the supplemental material.

Statistical analysis. A one-way analysis of variance (ANOVA) followed by a *post hoc* Dunnett's test for pairwise comparison was performed to compare the treated groups and the buffer-treated groups. A *P* value of <0.05 was considered statistically significant. Statistical analysis was performed with GraphPad Prism (version 5) software.

RESULTS

Generation and production of ALX-0171. The development of a *Pichia pastoris* strain for the production of ALX-0171 delivered a stable recombinant strain suitable for the manufacture of the multivalent trimeric ALX-0171 Nanobody. Further streamlining of the typical *Pichia pastoris* fermentation process resulted in an

TABLE 1 Affinities of ALX-0171, Nb017, and palivizumab toward RSV prefusion F protein measured by SPR

Compound	k_{on} ($M^{-1} s^{-1}$ [10^6])	k_{off} (s^{-1} [10^{-4}])	K_D (nM)	R_{max} (RU)	χ^2 (RU ²)
Nb017	1.305	233.5	17.880	14.73	0.713
ALX-0171	4.091	4.604	0.113	24.30	0.46
Palivizumab	0.084	0.739	0.879	56.2	0.0947
Fab D25	0.488	0.331	0.068	51.78	0.158
Fab 2F			>20		

ALX-0171 upstream process in which more than 7.5 g/liter ALX-0171 was secreted in the fermentation broth. After clarification of the broth, the downstream process consisted of capture, intermediate purification, and polish chromatography steps and was followed by a final formulation step. A range of ALX-0171 concentrations was tested in combination with a series of buffers and excipients to provide the highest stability after storage, nebulization, freeze-thaw, etc. These formulation and (stressed) stability studies resulted in the formulation of ALX-0171 as a stable nebulizer solution.

Characteristics of ALX-0171 binding to RSV F protein. The kinetics of Nb017 and ALX-0171 binding to the RSV F protein in its prefusion conformation was assessed by SPR analysis. The conformational integrity of the F protein was confirmed with the antigenic site \emptyset -specific Fab D25, which bound only to the prefusion conformation, whereas the antigenic site I-specific Fab 2F did not bind to the prefusion conformation, as expected. The binding affinity of palivizumab was 0.88 nM on the prefusion conformation, which is in a range similar to that of previously reported data (22, 32) (Table 1). Although Nanobody Nb017 was originally selected for binding to the RSV F protein in its postfusion conformation, as this was the only tool available at the time, both ALX-0171 and Nb017 were shown to bind the prefusion conformation of the F protein. The formatting of Nb017 into trimeric ALX-0171 increased the binding affinity by ~160-fold (K_D , 0.113 nM) compared to that of the monovalent Nb017 (K_D , 17.88 nM) (Table 1).

Formatting to ALX-0171 greatly increased *in vitro* potency against RSV-A and RSV-B. Microneutralization assays were used to investigate whether trimeric formatting of Nb017 (ALX-0171) would improve the neutralization capacity. The monovalent and trivalent formats inhibited the replication of the RSV-A (Long) and RSV-B (18537) strains in a dose-dependent manner (Fig. 1). Formatting of the monovalent building block into a trivalent compound greatly increased the potency by roughly 6,000-fold

against RSV-A Long and >10,000-fold against RSV-B 18537. ALX-0171 was 126- and 6-fold more potent than palivizumab against RSV-A Long and RSV-B 18537, respectively (Table 2). This increased potency of ALX-0171 over the potencies of the monovalent Nb017 and palivizumab was considerably more than anticipated on the basis of affinity differences. Similarly, the conversion of palivizumab Fab to full-length IgG resulted in an improved potency of ~200-fold with only a marginal <5-fold increase in K_D (22, 33).

ALX-0171 neutralizes a wide panel of clinical RSV isolates. The neutralization capacity of ALX-0171 toward RSV clinical isolates was tested. For this evaluation, 3 RSV-A strains isolated at Queen’s University Belfast, Belfast, Northern Ireland, United Kingdom, and 3 RSV-B strains isolated at the Baylor College of Medicine, Houston, TX, were selected. The 50% virus neutralization titers (as determined by endpoint dilution assays) are shown in Table 2. ALX-0171 was \geq 180-fold more potent than palivizumab against the RSV-A clinical isolates tested (range, 180- to 409-fold) and \geq 12-fold more potent than palivizumab against the RSV-B clinical isolates tested (range, 11.5- to 647.5-fold), and this potency difference was in the same range as that determined for the prototypic RSV-A Long and RSV-B 18537 strains (177- and 17-fold, respectively) using the same assay.

To provide a more comprehensive understanding of the relative neutralization capacity of ALX-0171 and palivizumab against a large panel of RSV clinical isolates, 61 RSV isolates, including the RSV Tracy and RSV-B 18537 strains (see Table S1 in the supplemental material), were tested for inhibition by ALX-0171 and palivizumab at a single concentration of 40 μ g/ml in a semiquantitative plaque reduction assay. This concentration represents the mean 30-day trough serum concentration of palivizumab after the first intramuscular injection (32). ALX-0171 and palivizumab reduced the viral titers by 2 \log_{10} for 97% and 85% of viruses tested, respectively (Table 3). For RSV-A isolates, this proportion was

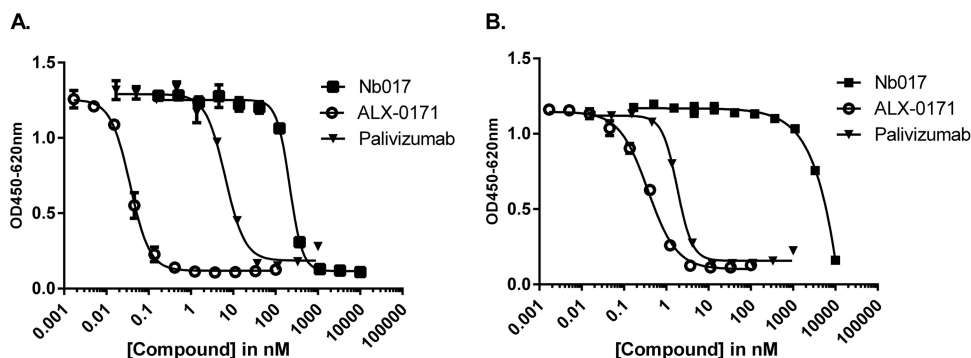


FIG 1 Microneutralization assay with ALX-0171, Nb017, and palivizumab. The capacities of ALX-0171, Nb017, and palivizumab to neutralize RSV-A Long (A) and RSV-B 18537 (B) were tested. The results shown depict the means of triplicate values \pm SEs. OD, optical density.

TABLE 2 Neutralization of RSV prototypic and clinical isolates^a

RSV strain	IC ₅₀			VN ₅₀		
	Mean ± SD IC ₅₀ (nM)		Fold difference	Mean ± SD VN ₅₀ (nM)		Fold difference
	ALX-0171	Palivizumab		ALX-0171	Palivizumab	
RSV-A						
Long	0.1 ± 0.07 (n = 3)	12.6 ± 5.4 (n = 3)	126	0.03 ± 0.02 (n = 3)	5.2 ± 0.8 (n = 3)	177
BT2a ^b				0.011 ± 0.006 (n = 3)	4.06 ± 1.39 (n = 3)	380
BT3a ^b				0.01 ± 0.005 (n = 3)	3.95 ± 0.61 (n = 3)	409
BT4a ^b				0.006 ± 0.006 (n = 3)	1.14 ± 0.91 (n = 3)	180
RSV-B						
18537	0.4 ± 0.2 (n = 20)	2.4 ± 1.2 (n = 5)	6	0.42 ± 0.66 (n = 6)	7.17 ± 5.52 (n = 6)	17
B-TX-60567 ^b				0.24 ± 0.22 (n = 3)	2.8 ± 0.8 (n = 3)	11.5
B-TX-61406 ^b				0.028 ± 0.026 (n = 3)	2.0 ± 1.1 (n = 3)	72.3
B-TX-79233 ^b				0.003 ± 0.001 (n = 3)	1.7 ± 2.2 (n = 3)	647.5

^a IC₅₀, 50% inhibitory concentration; VN₅₀, 50% virus neutralization titer; n, number of isolates.

^b These viruses have been reported previously (30, 31).

100% with ALX-0171 and 84.4% with palivizumab ($P = 0.053$), and for RSV-B isolates, this proportion was 93.1% with ALX-0171 and 86.2% with palivizumab ($P = 0.67$). These results are consistent with published data demonstrating that palivizumab neutralized 75/77 (97%) clinical isolates tested (32). Importantly, ALX-0171 demonstrated a broad RSV strain neutralization capacity that was at least as extensive as that of palivizumab when looking at 2 log₁₀ reductions.

Our data were the most striking when the complete suppression of RSV replication was compared between ALX-0171 and palivizumab. When they were tested at equivalent concentrations, ALX-0171 completely blocked replication in 87% of the viruses tested, whereas palivizumab completely blocked replication in 18% ($P < 0.0001$). This difference between ALX-0171 and palivizumab, which is likely the consequence of the higher potency of ALX-0171 (as shown in Table 2) and the lower molecular weight of ALX-0171 compared with that of full-length MAbs (42.2 for ALX-0171 versus 148 for palivizumab [32]), is indicative of a lower neutralization threshold for ALX-0171 than for palivizumab.

ALX-0171 binds to antigenic site II of F protein. To identify the residues that are important for the binding of ALX-0171 to RSV F protein, studies of the binding of monovalent Nb017 to RSV-A Long escape mutants containing a single point mutation in antigenic site II or IV were performed (Fig. 2). These tested RSV escape mutants, which are listed in Table 4, were previously re-

ported and selected with monoclonal antibodies to these sites (11, 28, 29). The binding of Nb017 to antigenic site II, but not site IV, mutants was significantly reduced (Table 4). In addition, binding of ALX-0171 to the RSV F protein competed with that of palivizumab, although only partially (Fig. 3 and data not shown). These results provide further evidence that Nb017 and, consequently, ALX-0171 target antigenic site II of the F protein and that its epitope is close to or overlaps that of palivizumab.

ALX-0171 retains physicochemical properties following nebulization. As the intended route of ALX-0171 administration is by inhalation, it is important that ALX-0171 withstand the nebulization process. An Akita² Apixneb nebulizer was used to nebulize ALX-0171, and the collected aerosol was characterized for product stability by size-exclusion (SE) high-pressure liquid chromatography (HPLC) (to determine purity/impurity), reverse-phase (RP)-HPLC (to determine purity), and ELISA (to determine potency). These analytical methods were suitable for assessing higher-molecular-weight product-related variants (i.e., dimeric, trimeric, and higher-multimer forms of ALX-0171), protein fragmentation, and potential changes in potency. During product development, no physicochemical changes were observed by RP-HPLC analysis after nebulization. SE-HPLC analysis showed a small increase in higher-molecular-weight species after nebulization. The formation of higher-molecular-weight species by nebulization was monitored during long-term stability studies and remained minimal, not exceeding 2% after nebulization.

TABLE 3 Comparative inhibition of *in vitro* replication of a panel of RSV clinical isolates by palivizumab and ALX-0171 by ≥100-fold or completely

RSV group	GMT ^a (log ₁₀)	No. of isolates with a ≥100-fold reduction/total no. of isolates tested (%)		P value ^b	No. of isolates with complete inhibition/total no. of isolates tested (%) ^c		P value
		Palivizumab	ALX-0171		Palivizumab	ALX-0171	
RSV-A	4.9 ± 0.4	27/32 (84.4)	32/32 (100)	0.053	0/32 (0)	30/32 (93.8)	<0.0001
RSV-B	4.7 ± 0.4	25/29 (86.2)	27/29 (93.1)	0.67	11/29 (37.9)	23/29 (79.3)	0.003
Total		52/61 (85.2)	59/61 (96.7)	0.054	11/61 (18)	53/61 (86.9)	<0.0001

^a GMT, geometric mean titer of buffer controls.

^b Differences between groups were analyzed using Fisher's exact test for comparison of proportions. Significance was defined at a P value of <0.05.

^c Complete virus inhibition was defined as no detectable virus plaques. The limit of virus detection in the plaque reduction neutralization assay was 5 PFU/ml.

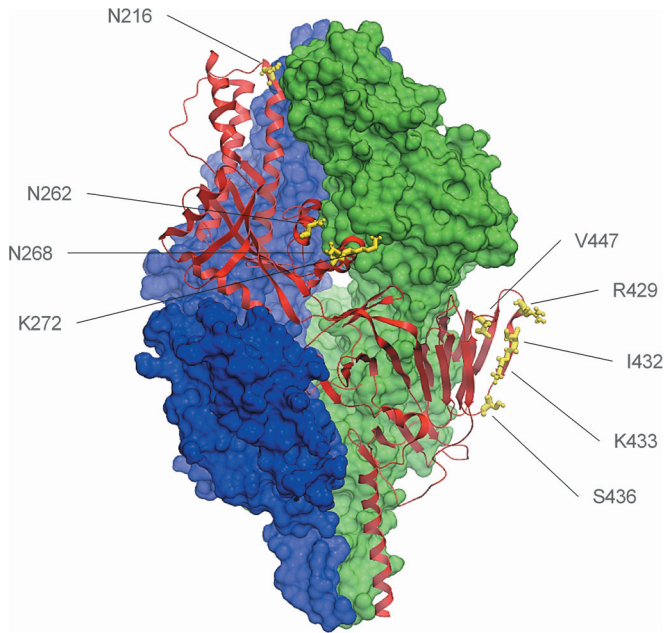


FIG 2 Crystal structure representation of the F protein in its prefusion conformation. Ribbon representation of one prefusion F-protein protomer is shown in red, and the other two protomers are shown in surface representation in blue and green. The residues listed are those that were mutated in the tested RSV escape mutants and are shown in yellow. The figure was prepared by using ICM Molsoft (46) and was derived from the sequence with PDB accession number 4JHW (26).

Furthermore, no effect of nebulization on ALX-0171 potency was observed by ELISA analysis (see Table S2 in the supplemental material).

Local delivery of ALX-0171 to cotton rats reduces the RSV load in the nose and lung. Cotton rats were used to evaluate the *in vivo* efficacy of ALX-0171 against RSV. Different doses of ALX-0171 were administered via the intranasal route on different days after RSV Tracy challenge either once (day 2 or day 3) or twice (day 2 and day 3) or by nebulization 1 h before RSV Tracy chal-

TABLE 4 Binding reactivity of Nb017 to membrane extracts of cells infected with distinct RSV-A Long escape mutants^a

RSV mutant	Amino acid substitution(s)	Antigenic site	% Nb017 binding ^b
R47F/4	N262Y	II	1.4 ± 1.6
R47F/7	N268I	II	61.1 ± 17.2
RAK13/4	N216D/N262Y	II	0.6 ± 0.8
R7C2/11	K272T	II	19.5 ± 16.8
R7C2/1	K272E	II	0.9 ± 1.1
R7.936/1	V447A	IV	119.9 ± 37.3
R7.936/4	K433T	IV	122.3 ± 40.5
R7.936/6	I432T	IV	106.5 ± 15.9
R9.432/1	S436F	IV	121.4 ± 20.0
RRA3	N262Y/R429S	II and IV	1.6 ± 3.2

^a Absorbance results were normalized to those for a reference Nanobody recognizing antigenic site I (191C7) with preserved binding to all depicted mutants to account for the difference in F-protein expression. Nb017 was used at 0.2 µg/ml.

^b Data represent the percent binding to that of the reference RSV-A Long wild-type strain ± standard deviation. Shading and boldface indicate where the binding of Nb017 was >75%, shading indicates where the binding of Nb017 was 25 to 75%, and no shading indicates where the binding of Nb017 was <25%.

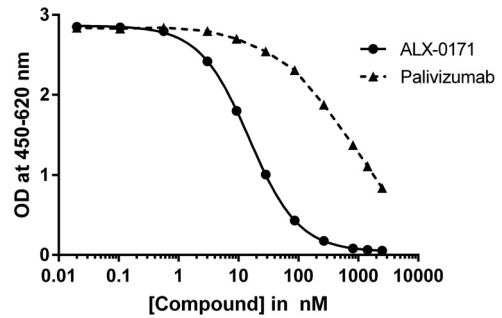


FIG 3 Results of competitive-binding ELISAs. The inhibition concentration-response curves obtained when biotinylated ALX-0171 was incubated with increasing concentrations of either unlabeled ALX-0171 or palivizumab are shown. The results shown depict the means of triplicate values ± SEs.

lenge (Table 5). On day 4 the cotton rats were sacrificed and the viral titers in both the nose and lung were determined.

Intranasal administration of ALX-0171 on day 2, day 3, or days 2 and 3 after RSV challenge resulted in significant viral load reductions in the lungs ranging from ~50-fold (1.66 log₁₀) for the lowest dose tested (1 mg/kg) (*P* < 0.0001) to ~2,000-fold (3.3 log₁₀) for the highest dose tested (68 mg/kg) (*P* < 0.0001). Nasal RSV titers were also significantly reduced for all doses and schedules tested (*P* < 0.0001), except for the day 2 treatment at 4 mg/kg (*P* = 0.7).

As the intended route of delivery of ALX-0171 is by nebulization, we performed a proof-of-concept experiment to confirm that nebulization did not affect the antiviral activity of ALX-0171. For this experiment, prophylactic delivery of ALX-0171 via nebulization was chosen as the most straightforward approach. In total, 4 groups of 6 cotton rats received estimated delivered doses of 0.3 mg/kg, 0.8 mg/kg, and 2 mg/kg 1 h before RSV Tracy challenge (Table 5). A dose-dependent reduction in viral titers was seen in the nose, which was significant for the two higher doses (*P* = 0.01 and 0.006 for doses of 0.8 mg/kg and 2 mg/kg, respectively). Furthermore, RSV replication was almost completely blocked in the lungs, even at the lowest dose tested (>3.67 log₁₀ reduction, *P* < 0.0001).

DISCUSSION

ALX-0171 is a novel therapeutic biologic in development for the treatment of RSV infections in infants. ALX-0171 is a trimeric Nanobody that binds an epitope in antigenic site II of RSV F protein with subnanomolar affinity. This epitope partially overlaps the palivizumab epitope.

The formatting of the monovalent Nb017 into the trivalent Nanobody ALX-0171 increased the potency of neutralization (>6,000-fold) of both RSV-A and RSV-B strains. Although formatting clearly increased the binding affinity for the biologically relevant prefusion conformation of the F protein (~160-fold), it does not fully explain the observed large increase in the virus neutralization capacity of ALX-0171. Our results are consistent with those of a previous report demonstrating that a bivalent Nanobody construct specific for F-protein antigenic site II had a 4,000-fold improved neutralization capacity compared to that of the monovalent construct against RSV-A Long (22). Likewise, the difference in potency between palivizumab Fab and the full-length antibody is 100-fold, while there is only a minimal improvement

TABLE 5 Reduction in RSV replication in cotton rats^a

Expt no., route of delivery	ALX-0171 dose delivered (mg/kg)	Treatment regimen	Nasal titer		Lung titer	
			Mean log ₁₀ total no. of PFU (±SD)	Log ₁₀ reduction vs buffer	Mean log ₁₀ no. of PFU/g lung (±SD)	Log ₁₀ reduction vs buffer
Expt 1, intranasal	Buffer	Days +2 and +3	4.78 (0.40)		4.94 (0.13)	
	1	Days +2 and +3	3.46 (0.56)	1.32*	3.28 (0.40)	1.66*
	2	Days +2 and +3	3.06 (0.75)	1.72*	3.14 (0.53)	1.81*
	4	Days +2 and +3	2.53 (0.88)	2.26*	3.18 (0.43)	1.76*
	21	Days +2 and +3	1.68 (0.28)	3.10*	2.05 (0.66)	2.89*
Expt 2, intranasal	Buffer	Days +2 and +3	4.84 (0.15)		5.19 (0.24)	
	4	Days +2 and +3	2.00 (0.72)	2.84*	2.04 (0.47)	3.15*
	19	Days +2 and +3	1.73 (0.21)	3.31*	2.55 (1.13)	2.64*
	68	Days +2 and +3	1.54 (0.59)	3.30*	1.88 (0.50)	3.30*
Expt 3, intranasal	Buffer	Days +2 and +3	4.81 (0.36)		4.88 (0.34)	
	4	Day +2	4.53 (0.87)	0.28	2.88 (0.89)	2.00*
	4	Day +3	1.84 (0.38)	2.97*	2.10 (0.22)	2.78*
	5	Days +2 and +3	1.74 (0.30)	3.07*	2.72 (1.12)	2.16*
Expt 4, nebulization	Buffer ^b	Hour -1	5.04 (0.25)		5.05 (0.22)	
	0.3 ^b	Hour -1	3.97 (0.62)	1.07	1.26 (0.34)	3.79*
	0.8 ^b	Hour -1	3.02 (1.46)	2.02*	1.38 (0.43)	3.67*
	2 ^b	Hour -1	2.87 (1.42)	2.18*	1.09 (0.05)	3.96*

^a Cotton rats (6 to 8 rats per group) were challenged with 1.41×10^5 to 3.4×10^5 PFU of RSV Tracy (intranasally, 100 μ l) on day 0. The animals received ALX-0171 at the indicated times either by intranasal administration or by nebulization. Viral titers and viral RNA loads in both the lung and nose were assessed on day 4 postinfection. *, $P < 0.05$ versus buffer control. *P* values were determined by ANOVA with a follow-up Dunnett's pairwise comparison test.

^b The delivered dose was estimated. The estimated delivered dose was defined as the estimated dose that is inhalable by the cotton rats and was calculated using the following formula: delivered dose (in micrograms per kilogram of body weight) = (aerosol concentration [in micrograms per liter]) \times (minute volume [in liters-minute per kilogram]) \times (treatment time [in minutes]) \times percentage of particles of $\leq 5 \mu$ m (respirable fraction), where the minute volume was estimated to be 0.7 liter-min/kg (47) and the respirable fraction was estimated to be 80% on the basis of the characteristics of the nebulizer.

in the K_D (33). However, the basis of this observation is not yet understood, and the precise mechanisms involved remain under investigation.

Like palivizumab, Nanobodies Nb017 and ALX-0171 bind to both the postfusion and prefusion conformation of the F protein and, as a result, likely inhibit the conformational changes related to F-protein activation, as suggested for other Nanobodies and monoclonal antibodies specific for antigenic site II (21, 34–36). This hypothesis is supported by a model of the RSV F-protein prefusion structure, in which the residues of antigenic site II are proximal to sequences that form the central α -helical coil of the 6-helix bundles in the postfusion conformation of the F protein (35).

Importantly, the capacity of ALX-0171 to neutralize recent clinical isolates or prototypic strains greatly surpassed that of palivizumab in terms of both plaque reductions and the complete block of RSV infection. This increased inhibition efficiency was consistent with previous reports, in which the virus- and cell-cell fusion-inhibiting capacity of a bivalent Nanobody targeting F-protein antigenic site II was compared to that of palivizumab (21, 22). There are several possible explanations for this difference in neutralization capacity: (i) the smaller size of ALX-0171 and its extended complementarity-determining region loops may enhance the accessibility to F-protein antigenic site II (37, 38), (ii) the GS linker is likely more flexible than the hinge of a full-length antibody, and thus, ALX-0171 would be able to access its binding site more readily, and (iii) the trivalency of ALX-0171 may allow additional binding modes, such as simultaneous binding of three

independent F-protein trimers or simultaneous binding of the three subunits within a single F-protein trimer (20, 21), as the length of the GS linkers was specifically designed to allow such interactions. Further crystallography studies are needed to elucidate the mechanisms involved in this increased neutralization capacity of ALX-0171.

In vivo, ALX-0171 was shown to be highly efficient at reducing and/or blocking RSV replication in the lung and nose, similar to what was reported for motavizumab, an affinity-matured version of palivizumab (39, 40), whereas no effect on viral load in the nose was demonstrated for palivizumab at doses of ≤ 15 mg/kg (40, 41). There remains the possibility that the residual ALX-0171 present in the wash fluid interfered in the plaque assay. Nonetheless, despite this caveat, we believe that it remains the most valid assessment, as it reflects the fact either that less virus is present or that any virus still present is effectively neutralized. Importantly, as ALX-0171 is devoid of an Fc, its *in vivo* efficacy likely relies entirely on direct antiviral activity, in contrast to what has been reported for palivizumab (42). In addition and in contrast to the route of delivery of palivizumab and motavizumab, which were administered systemically in therapeutic trials in infants and demonstrated conflicting effects on nasal/tracheal viral loads (39, 41, 43), ALX-0171 is delivered straight to the site of infection. Direct administration to the airways is likely to provide faster and more robust antiviral activity in the respiratory tract, which may be critical for the treatment of an acute disease like RSV infection. Indeed, the therapeutic effect of topical administration of purified human immunoglobulins, screened for high RSV neutralization

activity, resulting in a decrease in viral loads in cotton rats was shown to be 160 times greater than that by administration by the parenteral route (44). In addition to the greater effectiveness of the ALX-0171 administration route, the neutralization threshold of ALX-0171 (i.e., the expected lung concentration needed to exert the full antiviral effect) is also anticipated to be lower than that of palivizumab. This is particularly important in a clinical setting where the administered dose is a limiting factor.

In summary, ALX-0171 represents a novel, highly potent antiviral with broad specificity toward a large panel of RSV clinical isolates and may have significant potential for therapeutic use. Furthermore, direct delivery of ALX-0171 to the airways/lungs by nebulization proved an effective mode of drug delivery, as even the lowest dose of only 1 mg/kg delivered intranasally still showed antiviral efficacy. As nebulization has been shown to result in fast and efficient drug delivery to the principal site of RSV infection (45), i.e., the upper and lower respiratory tract, this mode of drug delivery may provide major therapeutic advantages for ALX-0171 in treating RSV-infected patients.

ACKNOWLEDGMENTS

We thank Valerie Lambert, Maureen Van den Hemel, Jorn Audiens, and Ananza Vanderrijst for their technical support and expertise, Veronique De Brabandere and her team for the Nanobody physicochemical characterization, Erika Morizzo for providing the structural model of the prefusion F protein, and Hans Ulrichs and his team for fruitful scientific discussions. We also thank Vectura GmbH for the supply of the nebulizers.

L.D., C.S., K.A., and E.D. are all current employees of Ablynx; all employees own stock/stock options of Ablynx. T.S. was an employee of Ablynx at the time of data generation. C.P., P.A.P., B.E.G., V.M., A.M., U.F.P. and J.A.M. undertook this work as part of a research contract with Ablynx.

The terms “Nanobody” and “Nanobodies” are registered trademarks of Ablynx nv.

FUNDING INFORMATION

This work was supported by the Agentschap voor Innovatie door Wetenschap en Techniek (IWT), Belgium (grant numbers 100333 and 130562). Work in Madrid was partially supported by grant SAF2012-31217 to J.A.M. from Plan Nacional I+D+I.

REFERENCES

- Nair H, Nokes DJ, Gessner BD, Dherani M, Madhi SA, Singleton RJ, O'Brien KL, Roca A, Wright PF, Bruce N, Chandran A, Theodoratou E, Sutanto A, Sedyaningsih ER, Ngama M, Munywoki PK, Kartasasmita C, Simoes EA, Rudan I, Weber MW, Campbell H. 2010. Global burden of acute lower respiratory infections due to respiratory syncytial virus in young children: a systematic review and meta-analysis. *Lancet* 375:1545–1555. [http://dx.doi.org/10.1016/S0140-6736\(10\)60206-1](http://dx.doi.org/10.1016/S0140-6736(10)60206-1).
- Zhang L, Peeples ME, Boucher RC, Collins PL, Pickles RJ. 2002. Respiratory syncytial virus infection of human airway epithelial cells is polarized, specific to ciliated cells, and without obvious cytopathology. *J Virol* 76:5654–5666. <http://dx.doi.org/10.1128/JVI.76.11.5654-5666.2002>.
- Villeneuve R, Thavagnanam S, Sarlang S, Parker J, Douglas I, Skibinski G, Heaney LG, McKaigue JP, Coyle PV, Shields MD, Power UF. 2012. In vitro modeling of respiratory syncytial virus infection of pediatric bronchial epithelium, the primary target of infection in vivo. *Proc Natl Acad Sci U S A* 109:5040–5045. <http://dx.doi.org/10.1073/pnas.1110203109>.
- Aliyu A, Ahmad A, Rogo L, Sale J, Idris H. 2010. Biology of human respiratory syncytial virus: a review. *Bayero J Pure Appl Sci* 3:147–155.
- Backman K, Piippo-Savolainen E, Ollikainen H, Koskela H, Korppi M. 2014. Adults face increased asthma risk after infant RSV bronchiolitis and reduced respiratory health-related quality of life after RSV pneumonia. *Acta Paediatr* 103:850–855. <http://dx.doi.org/10.1111/apa.12662>.
- Wennergren G, Kristjansson S. 2001. Relationship between respiratory

syncytial virus bronchiolitis and future obstructive airway diseases. *Eur Respir J* 18:1044–1058. <http://dx.doi.org/10.1183/09031936.01.00254101>.

- Mejias A, Ramilo O. 2008. Review of palivizumab in the prophylaxis of respiratory syncytial virus (RSV) in high-risk infants. *Biologics* 2:433–439.
- Wu H, Pfarr DS, Losonsky GA, Kiener PA. 2008. Immunoprophylaxis of RSV infection: advancing from RSV-IGIV to palivizumab and motavizumab. *Curr Top Microbiol Immunol* 317:103–123.
- The IMPact-RSV Study Group. 1998. Palivizumab, a humanized respiratory syncytial virus monoclonal antibody, reduces hospitalization from respiratory syncytial virus infection in high-risk infants. *Pediatrics* 102:531–537. <http://dx.doi.org/10.1542/peds.102.3.531>.
- American Academy of Pediatrics Committee on Infectious Diseases, American Academy of Pediatrics Bronchiolitis Guidelines Committee. 2014. Updated guidance for palivizumab prophylaxis among infants and young children at increased risk of hospitalization for respiratory syncytial virus infection. *Pediatrics* 134:415–420. <http://dx.doi.org/10.1542/peds.2014-1665>.
- Lopez JA, Bustos R, Orvell C, Berois M, Arbiza J, Garcia-Barreno B, Melero JA. 1998. Antigenic structure of human respiratory syncytial virus fusion glycoprotein. *J Virol* 72:6922–6928.
- Black CP. 2003. Systematic review of the biology and medical management of respiratory syncytial virus infection. *Respir Care* 48:209–231.
- Peret TC, Hall CB, Schnabel KC, Golub JA, Anderson LJ. 1998. Circulation patterns of genetically distinct group A and B strains of human respiratory syncytial virus in a community. *J Gen Virol* 79(Pt 9):2221–2229.
- Venter M, Madhi SA, Tiemessen CT, Schoub BD. 2001. Genetic diversity and molecular epidemiology of respiratory syncytial virus over four consecutive seasons in South Africa: identification of new subgroup A and B genotypes. *J Gen Virol* 82:2117–2124. <http://dx.doi.org/10.1099/0022-1317-82-9-2117>.
- Eshaghi A, Duvvuri VR, Lai R, Nadarajah JT, Li A, Patel SN, Low DE, Gubbay JB. 2012. Genetic variability of human respiratory syncytial virus A strains circulating in Ontario: a novel genotype with a 72 nucleotide G gene duplication. *PLoS One* 7:e32807. <http://dx.doi.org/10.1371/journal.pone.0032807>.
- Shobugawa Y, Saito R, Sano Y, Zaraket H, Suzuki Y, Kumaki A, Daput I, Oguma T, Yamaguchi M, Suzuki H. 2009. Emerging genotypes of human respiratory syncytial virus subgroup A among patients in Japan. *J Clin Microbiol* 47:2475–2482. <http://dx.doi.org/10.1128/JCM.00115-09>.
- Avadhanula V, Chemaly RF, Shah DP, Ghantaji SS, Azzi JM, Aideyan LO, Mei M, Piedra PA. 2015. Infection with novel respiratory syncytial virus genotype Ontario (ON1) in adult hematopoietic cell transplant recipients, Texas, 2011–2013. *J Infect Dis* 211:582–589. <http://dx.doi.org/10.1093/infdis/jiu473>.
- Hamers-Casterman C, Atarhouch T, Muyldermans S, Robinson G, Hamers C, Songa EB, Bendahman N, Hamers R. 1993. Naturally occurring antibodies devoid of light chains. *Nature* 363:446–448. <http://dx.doi.org/10.1038/363446a0>.
- Van Bockstaele F, Holz JB, Revets H. 2009. The development of Nanobodies for therapeutic applications. *Curr Opin Investig Drugs* 10:1212–1224.
- Vanlandschoot P, Stortelers C, Beirnaert E, Ibanez LI, Schepens B, Depla E, Saelens X. 2011. Nanobodies(R): new ammunition to battle viruses. *Antiviral Res* 92:389–407. <http://dx.doi.org/10.1016/j.antiviral.2011.09.002>.
- Schepens B, Ibanez LI, De Baets S, Hultberg A, Bogaert P, De Bleser P, Vervalle F, Verrips T, Melero J, Vandeveldel W, Vanlandschoot P, Saelens X. 2011. Nanobodies(R) specific for respiratory syncytial virus fusion protein protect against infection by inhibition of fusion. *J Infect Dis* 204:1692–1701. <http://dx.doi.org/10.1093/infdis/jir622>.
- Hultberg A, Temperton NJ, Rosseels V, Koenders M, Gonzalez-Pajuelo M, Schepens B, Ibanez LI, Vanlandschoot P, Schillemans J, Saunders M, Weiss RA, Saelens X, Melero JA, Verrips CT, Van Gucht S, de Haard HJ. 2011. Llama-derived single domain antibodies to build multivalent, superpotent and broadened neutralizing anti-viral molecules. *PLoS One* 6:e17665. <http://dx.doi.org/10.1371/journal.pone.0017665>.
- National Institutes of Health. 18 June 2015, posting date. A multicentre study in otherwise healthy infants and toddlers hospitalized for and diagnosed with RSV lower respiratory tract infection to evaluate the safety, tolerability, and clinical activity of ALX-0171. National Institutes of Health, Bethesda, MD.

24. Corral T, Ver LS, Mottet G, Cano O, Garcia-Barreno B, Calder LJ, Shehel JJ, Roux L, Melero JA. 2007. High level expression of soluble glycoproteins in the allantoic fluid of embryonated chicken eggs using a Sendai virus minigenome system. *BMC Biotechnol* 7:17. <http://dx.doi.org/10.1186/1472-6750-7-17>.
25. Kwakkenbos MJ, Diehl SA, Yasuda E, Bakker AQ, van Geelen CM, Lukens MV, van Bleek GM, Widjojoatmodjo MN, Bogers WM, Mei H, Radbruch A, Scheeren FA, Spits H, Beaumont T. 2010. Generation of stable monoclonal antibody-producing B cell receptor-positive human memory B cells by genetic programming. *Nat Med* 16:123–128. <http://dx.doi.org/10.1038/nm.2071>.
26. McLellan JS, Chen M, Leung S, Graepel KW, Du X, Yang Y, Zhou T, Baxa U, Yasuda E, Beaumont T, Kumar A, Modjarrad K, Zheng Z, Zhao M, Xia N, Kwong PD, Graham BS. 2013. Structure of RSV fusion glycoprotein trimer bound to a prefusion-specific neutralizing antibody. *Science* 340:1113–1117. <http://dx.doi.org/10.1126/science.1234914>.
27. Garcia-Barreno B, Palomo C, Penas C, Delgado T, Perez-Brena P, Melero JA. 1989. Marked differences in the antigenic structure of human respiratory syncytial virus F and G glycoproteins. *J Virol* 63:925–932.
28. Arbiza J, Taylor G, Lopez JA, Furze J, Wyld S, Whyte P, Stott EJ, Wertz G, Sullender W, Trudel M, Melero JA. 1992. Characterization of two antigenic sites recognized by neutralizing monoclonal antibodies directed against the fusion glycoprotein of human respiratory syncytial virus. *J Gen Virol* 73(Pt 9):2225–2234. <http://dx.doi.org/10.1099/0022-1317-73-9-2225>.
29. Melero JA, Moore ML. 2013. Influence of respiratory syncytial virus strain differences on pathogenesis and immunity. *Curr Top Microbiol Immunol* 372:59–82. http://dx.doi.org/10.1007/978-3-642-38919-1_3.
30. Villenave R, O'Donoghue D, Thavagnanam S, Touzelet O, Skibinski G, Heaney LG, McKaigue JP, Coyle PV, Shields MD, Power UF. 2011. Differential cytopathogenesis of respiratory syncytial virus prototypic and clinical isolates in primary pediatric bronchial epithelial cells. *Virol J* 8:43. <http://dx.doi.org/10.1186/1743-422X-8-43>.
31. Tapia LI, Shaw CA, Aideyan LO, Jewell AM, Dawson BC, Haq TR, Piedra PA. 2014. Gene sequence variability of the three surface proteins of human respiratory syncytial virus (HRSV) in Texas. *PLoS One* 9:e90786. <http://dx.doi.org/10.1371/journal.pone.0090786>.
32. European Medicines Agency. 2004. WC500056731 EPAR: initial scientific discussion for the approval of Synagis. European Medicines Agency, London, United Kingdom.
33. Wu H, Pfarr DS, Tang Y, An LL, Patel NK, Watkins JD, Huse WD, Kiener PA, Young JF. 2005. Ultra-potent antibodies against respiratory syncytial virus: effects of binding kinetics and binding valence on viral neutralization. *J Mol Biol* 350:126–144. <http://dx.doi.org/10.1016/j.jmb.2005.04.049>.
34. Huang K, Incognito L, Cheng X, Ulbrandt ND, Wu H. 2010. Respiratory syncytial virus-neutralizing monoclonal antibodies motavizumab and palivizumab inhibit fusion. *J Virol* 84:8132–8140. <http://dx.doi.org/10.1128/JVI.02699-09>.
35. Magro M, Andreu D, Gomez-Puertas P, Melero JA, Palomo C. 2010. Neutralization of human respiratory syncytial virus infectivity by antibodies and low-molecular-weight compounds targeted against the fusion glycoprotein. *J Virol* 84:7970–7982. <http://dx.doi.org/10.1128/JVI.00447-10>.
36. McLellan JS, Chen M, Kim A, Yang Y, Graham BS, Kwong PD. 2010. Structural basis of respiratory syncytial virus neutralization by motavizumab. *Nat Struct Mol Biol* 17:248–250. <http://dx.doi.org/10.1038/nsmb.1723>.
37. Desmyter A, Decanniere K, Muyldermans S, Wyns L. 2001. Antigen specificity and high affinity binding provided by one single loop of a camel single-domain antibody. *J Biol Chem* 276:26285–26290. <http://dx.doi.org/10.1074/jbc.M102107200>.
38. Muyldermans S, Cambillau C, Wyns L. 2001. Recognition of antigens by single-domain antibody fragments: the superfluous luxury of paired domains. *Trends Biochem Sci* 26:230–235. [http://dx.doi.org/10.1016/S0968-0004\(01\)01790-X](http://dx.doi.org/10.1016/S0968-0004(01)01790-X).
39. Lagos R, DeVincenzo JP, Munoz A, Hultquist M, Suzich J, Connor EM, Losonsky GA. 2009. Safety and antiviral activity of motavizumab, a respiratory syncytial virus (RSV)-specific humanized monoclonal antibody, when administered to RSV-infected children. *Pediatr Infect Dis J* 28:835–837. <http://dx.doi.org/10.1097/INF.0b013e3181a165e4>.
40. Wu H, Pfarr DS, Johnson S, Brewah YA, Woods RM, Patel NK, White WI, Young JF, Kiener PA. 2007. Development of motavizumab, an ultra-potent antibody for the prevention of respiratory syncytial virus infection in the upper and lower respiratory tract. *J Mol Biol* 368:652–665. <http://dx.doi.org/10.1016/j.jmb.2007.02.024>.
41. Malley R, DeVincenzo J, Ramilo O, Dennehy PH, Meissner HC, Gruber WC, Sanchez PJ, Jafri H, Balsley J, Carlin D, Buckingham S, Vernacchio L, Ambrosino DM. 1998. Reduction of respiratory syncytial virus (RSV) in tracheal aspirates in intubated infants by use of humanized monoclonal antibody to RSV F protein. *J Infect Dis* 178:1555–1561. <http://dx.doi.org/10.1086/314523>.
42. Hiatt A, Bohorova N, Bohorov O, Goodman C, Kim D, Pauly MH, Velasco J, Whaley KJ, Piedra PA, Gilbert BE, Zeitlin L. 2014. Glycan variants of a respiratory syncytial virus antibody with enhanced effector function and in vivo efficacy. *Proc Natl Acad Sci U S A* 111:5992–5997. <http://dx.doi.org/10.1073/pnas.1402458111>.
43. Ramilo O, Lagos R, Saez-Llorens X, Suzich J, Wang CK, Jensen KM, Harris BS, Losonsky GA, Griffin MP. 2014. Motavizumab treatment of infants hospitalized with respiratory syncytial virus infection does not decrease viral load or severity of illness. *Pediatr Infect Dis J* 33:703–709. <http://dx.doi.org/10.1097/INF.0000000000000240>.
44. Prince GA, Hemming VG, Horswood RL, Baron PA, Chanock RM. 1987. Effectiveness of topically administered neutralizing antibodies in experimental immunotherapy of respiratory syncytial virus infection in cotton rats. *J Virol* 61:1851–1854.
45. De Bruyn S, De Smedt T, Allosery K, Crabbe P, De Brabandere V, Detalle L, Mortier K, Schoolmeester A, Wouters H, Stöhr T, Depla E. 2015. ALX-0171: safety and therapeutic potential of an inhaled anti-RSV Nanobody. *RDD Europe* 2015 1:37–48.
46. Abagyan R, Totrov M. 1994. Biased probability Monte Carlo conformational searches and electrostatic calculations for peptides and proteins. *J Mol Biol* 235:983–1002. <http://dx.doi.org/10.1006/jmbi.1994.1052>.
47. Phalen R. 1984. Inhalation studies: foundations and techniques. CRC Press LLC, Boca Raton, FL.